

# Spin-Orbit Coupling Force for 14N Elastic Scattering

著者	Yamaya T., Satoh O., Morita S., Kotajima K., Shinozuka T., Fujioka M., Hirota J.I., Sato A.
journal or publication title	CYRIC annual report
volume	1984
page range	7-11
year	1984
URL	<a href="http://hdl.handle.net/10097/49206">http://hdl.handle.net/10097/49206</a>

I. 2 Spin-Orbit Coupling Force for  $^{14}\text{N}$  Elastic Scattering

Yamaya T., Satoh O., Morita S., Kotajima K.\*, Shinozuka T.\*\*, Fujioka M.\*\*,  
Hirota J.I. and Sato A.

Department of Physics, Faculty of Science, Tohoku University

Department of Nuclear Engineering, Tohoku University\*

Cyclotron and Radioisotope Center, Tohoku University\*\*

There has been considerable recent interest in the spin-orbit term in the heavy-ion optical potential. The elastic asymmetry has been measured for the scattering of polarized  $^6\text{Li}$  ions from several targets.<sup>1)</sup> A reasonable description of these data has been obtained using a theoretical spin orbit potential based on a single folding cluster model.<sup>2)</sup> A general double folding prescription is used in conjunction with a realistic G-matrix interaction to estimate the strength of the elastic spin-orbit potential for several heavy-ion systems. The potentials obtained give a reasonable description of the elastic asymmetry data. Kubono et al. have speculated that spin-orbit distortion might have important effects on the angular distributions for transfer reactions.<sup>3)</sup> In another experiment<sup>4)</sup>, significant back angle differences were noted in the elastic differential cross sections for  $^{10,11}\text{B}+^{27}\text{Al}$  at 50 MeV and  $^{12}\text{C}+^{27}\text{Al}$  at 55 MeV. These differences were largely attributed to quadrupole terms in the elastic scattering potentials; however, it was suggested that possible effects due to spin-orbit terms should also be investigated.

In heavy-ion elastic scattering data at relating low bombarding energies (<10 MeV per nucleon) which often are not very far above the Coulomb barrier, the scattering is sensitive to the potential in the vicinity of the strong absorption radius. In the elastic scattering of spin 1 heavy ion projectiles from spin 0 target nuclei, the total angular momentum of the projectiles are defined by  $j = \ell \pm 1$ ,  $\ell$ , where the sign depend on the orientation of the spin of the projectile relative to the orbital angular momentum  $\ell$ . In the general spin-orbit coupling interaction picture  $V_{\ell s}(r) < 0$  for  $j = \ell + 1$  and  $V_{\ell s}(r) > 0$  for  $j = \ell - 1$ . It is important to note the difference in sign between the spin-orbit coupling interactions in the region of the strong absorption radius. Projectiles distorted to be nearing the target nuclei by the negative spin-orbit interaction are more strongly absorbed, and on the contrary projectiles distorted to be far from the target nuclei by the positive spin-orbit interaction weaken the effect of absorption. A qualitative description is shown in Figure 1 as results of the calculations.

In order to obtain information of the angular distribution dependent on the projectile spin for the heavy-ion elastic scattering, we have measured the differential cross sections for the systems  $^{12}\text{C}+^{28}\text{Si}$ ,  $^{16}\text{O}+^{28}\text{Si}$  and  $^{14}\text{N}+^{28}\text{Si}$  at

angles  $\theta_{cm} < 70^\circ$  in step of  $\Delta\theta_{cm} \leq 1^\circ$ . The elastic and inelastic scattering angular distributions were obtained using the  $^{12}\text{C}$  beam of 65 MeV,  $^{16}\text{O}$  beam of 75 MeV and  $^{14}\text{N}$  beam of 84 MeV at the Tohoku University 680-cyclotron facility.<sup>5)</sup> For these measurements natural Si selfsupport targets of 100-180  $\mu\text{g}/\text{cm}^2$  thickness were used. The angular distributions were measured using a counter system which consists of two standard  $\Delta E$  surface barrier detectors and a position-sensitive surface barrier detector. This counter system has two telescopes  $\Delta E_1$ -E and  $\Delta E_2$ -E, where two  $\Delta E$  detectors were placed in a row along a surface of position sensitive detector. Each telescope has three slits and the spectra at six angles can be measured at the same time.

The ratio of the experimental differential cross sections to Rutherford scattering are shown in Fig. 2 together with results of the DWBA calculations. The optical model search code ELAST2<sup>6)</sup> was used to fit the data. On the other hand, data for  $^{16}\text{O}+^{28}\text{Si}$  scattering between 33 and 215 MeV have been fitted by the optical potential with a shallow potential whose real part had a depth of about 10 MeV, within the framework of an energy-independent six-parameter potential of Woods-Saxon form.<sup>7)</sup> These data have been also fitted by Satchler using optical potentials with deep, energy-independent, real parts provided the surface diffuseness of the imaginary part is allowed to increase slowly and linearly with bombarding energy.<sup>8)</sup>

The potentials of two types studied by Cramer et al.<sup>7)</sup> called by them A-23 which had  $V = 100$  MeV and E-18 which had  $V = 10$  MeV, have been applied for fitting the present data. However, the parameters were adjusted so as to get best fit to the present data. The parameters obtained from the present analysis are shown in Table 1 together with the parameters studied by Cramer et al. There are some discrepancies between optical model parameters of  $^{16}\text{O}+^{28}\text{Si}$  system obtained from present data at  $E = 75$  MeV and from the data at  $E = 81$  MeV by Cramer et al. This discrepancy originates in difference between the data, that is, the diffraction pattern which has not been observed by Cramer et al. was observed at forward angles in the present angular distribution. As shown in Table 1, in both of shallow and deep potential the optical model parameters for  $^{12}\text{C}$  projectile with spin 0 are in agreement with those for  $^{16}\text{O}$  projectile with spin 0. However, the optical model parameters for  $^{14}\text{N}$  projectile with spin 1 are markedly different from those for  $^{12}\text{C}$  and  $^{16}\text{O}$  projectiles. The dotted curve in Fig. 2 is the result of DWBA calculation in the  $^{14}\text{N}+^{28}\text{Si}$  system using the shallow potential including a spin-orbit term. The value of  $\chi^2$  per datum in this case is twice as large as the value in the E18-N1 potential case. However, the central potential parameters of the optical potential including the spin-orbit coupling force in the  $^{14}\text{N}+^{28}\text{Si}$  system are similar to those in the  $^{12}\text{C}+^{28}\text{Si}$  and the  $^{16}\text{O}+^{28}\text{Si}$  systems. On the basis of this result, it is suggested that the spin-orbit coupling force should be accounted for the elastic scattering of heavy with spin.

## References

- 1) Weiss W. et al., Phys. Lett. 61B (1976) 237.
- 2) Amakawa H. and Kubo K.I., Nucl. Phys. A266 (1976) 521.
- 3) Kubono S. et al., Phys. Rev. Lett. 38 (1977) 817.
- 4) Parks L. A., Kemper K. W. et al., Phys. Lett. 70B (1977) 27.
- 5) Yamaya T. et al., Nucl. Instr. and Meth. 203 (1982) 7, Nucl. Instr. and Meth. 226 (1984) 219.
- 6) Igarashi M., Optical model auto search code ELAST2 private communication.
- 7) Cramer J. G., Devries R. M., Goldberg D. A., Zisman M. S. and Maguire C. F., Phys. Rev. C 14 (1976) 2158.
- 8) Satchler G. R., Nucl. Phys. A279 (1977) 493.

Table 1. Optical potential parameters.

Potential	V (MeV)	$r_0$ (fm)	a (fm)	W (MeV)	$r_I$ (fm)	$a_I$ (fm)	$r_C$ (fm)	$V_{so}$ (MeV)	$r_{so}$ (fm)	$a_{so}$ (fm)	$\chi^2/N$
E-18 $^{16}_0$	10	1.35	0.618	23.4	1.23	0.552	—	—	—	—	
E18-C $^{12}_C$	10	1.397	0.424	20.96	1.279	0.350	1.0	—	—	—	40.9
E18-0 $^{16}_0$	10	1.44	0.375	20.96	1.312	0.319	1.0	—	—	—	7.89
E-18-N1 $^{14}_N$	32.58	1.19	0.625	8.623	1.330	0.681	1.0	—	—	—	55.2
E-18-N2 $^{14}_N$	14.4	1.373	0.520	21.2	1.282	0.350	1.0	0.162	1.778	0.679	125
A23 $^{16}_0$	100	0.932	0.797	165	0.89	0.764	—	—	—	—	
Atype $^{16}_0$	100	0.967	0.745	44.1	1.073	0.605	—	—	—	—	
A-C $^{12}_C$	89.76	1.059	0.604	20.71	1.145	0.625	1.3	—	—	—	37.9
A-0 $^{16}_0$	89.76	1.042	0.674	20.71	1.178	0.557	1.2	—	—	—	8.61
A-N $^{14}_N$	84.82	1.144	0.532	10.06	1.288	0.632	1.3	—	—	—	90.9

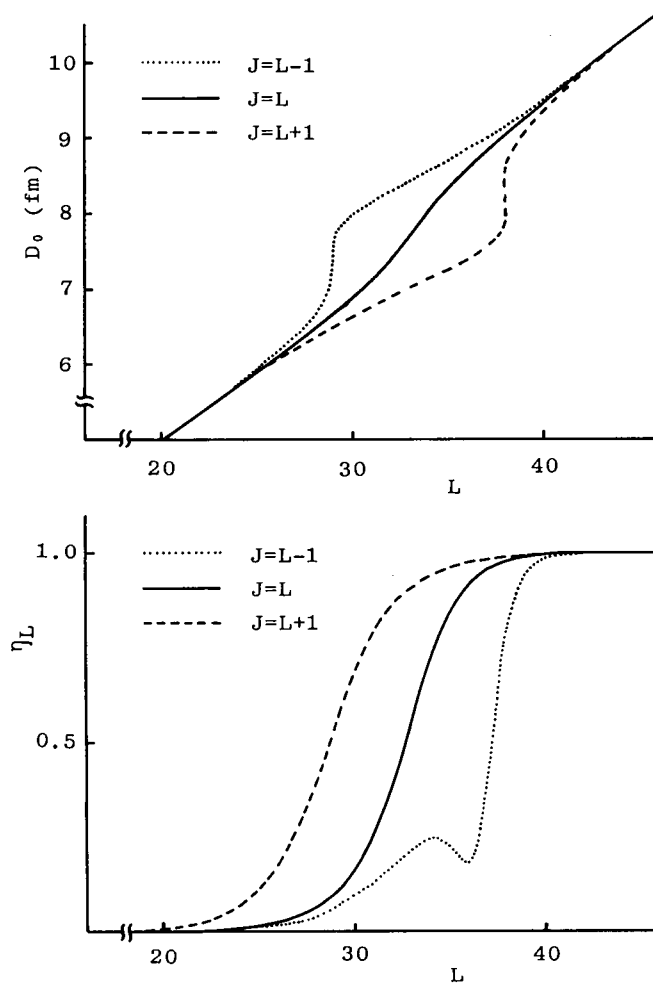


Fig. 1. Location of the turning points (top) and the scattering reflection coefficients (bottom) as a function of the partial angular momentum  $L$  for the total angular momentum  $j_{\pm} = L \pm 1$  and  $j = L$ .

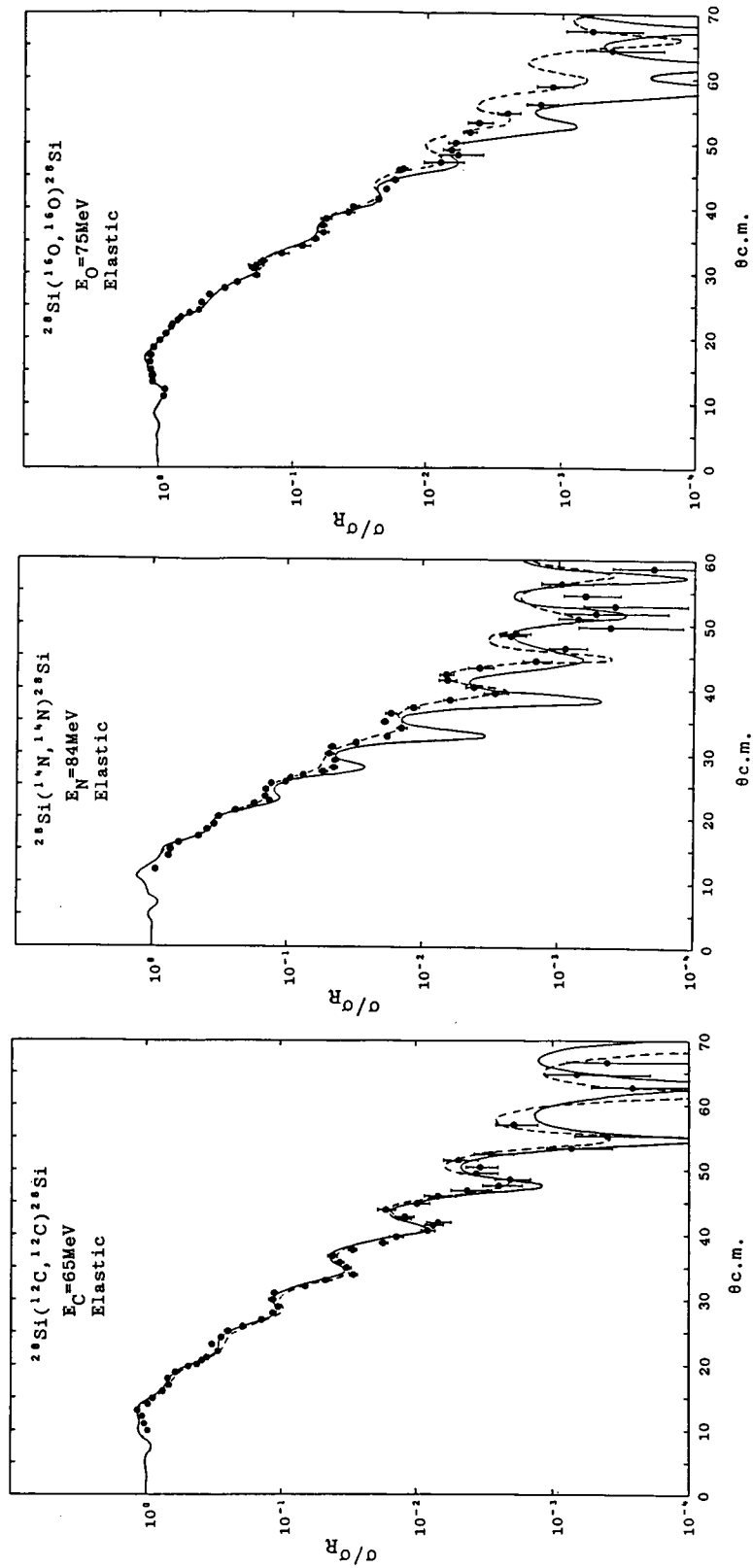


Fig. 2. Angular dependence of the ratio of the cross sections to Rutherford scattering in the systems of  $^{12}\text{C}+^{28}\text{Si}$ ,  $^{14}\text{N}+^{28}\text{Si}$  and  $^{16}\text{O}+^{28}\text{Si}$ . Solid and dotted curves indicate the results of the DWBA calculations for the shallow and deep potentials, respectively, in the  $^{12}\text{C}+^{28}\text{Si}$  and  $^{16}\text{O}+^{28}\text{Si}$  systems. In the  $^{14}\text{N}+^{28}\text{Si}$  system, solid and dotted curves indicate the results of the DWBA calculations for the shallow potential without and with a l-s coupling force, respectively.